Heliyon 8 (2022) e08827

Contents lists available at ScienceDirect

Heliyon

journal homepage: www.cell.com/heliyon

Research article

Connectivity and variability of related cognitive subregions lead to different stages of progression toward Alzheimer's disease

Jinhua Sheng [a,b,*], Bocheng Wang [a,b,c], Qiao Zhang [d,e], Margaret Yu [f]

[a] School of Computer Science, Hangzhou Dianzi University, Hangzhou, Zhejiang, 310018, China
[b] Key Laboratory of Intelligent Image Analysis for Sensory and Cognitive Health, Ministry of Industry and Information Technology of China, Hangzhou, Zhejiang, 310018, China
[c] Communication University of Zhejiang, Hangzhou, Zhejiang, 310018, China
[d] Beijing Hospital, Beijing, 100730, China
[e] Institute of Geriatric Medicine, Chinese Academy of Medical Sciences, Beijing, 100730, China
[f] Department of Neurology, Northwestern University Feinberg School of Medicine, Chicago, IL, 60611, USA

ARTICLE INFO

Keywords:
Multimodal cerebral cortical measures
Multimodal deep learning
Multi-group classification
Alzheimer's disease
Mild cognitive impairment

ABSTRACT

Single modality MRI data is not enough to depict and discern the cause of the underlying brain pathology of Alzheimer's disease (AD). Most existing studies do not perform well with multi-group classification. To reveal the structural, functional connectivity and functional topological relationships among different stages of mild cognitive impairment (MCI) and AD, a novel method was proposed in this paper for the analysis of regional importance with an improved deep learning model. Obvious drift of related cognitive regions can be observed in the prefrontal lobe and surrounding the cingulate area in the right hemisphere when comparing AD and healthy controls (HC) based on absolute weights in the classification mode. Alterations of these regions being responsible for cognitive impairment have been previously reported. Different parcellation atlases of the human cerebral cortex were compared, and the fine-grained multimodal parcellation HCPMMP performed the best with 180 cortical areas per hemisphere. In multi-group classification, the highest accuracy achieved was 96.86% with the utilization of structural and functional topological modalities as input to the training model. Weights in the trained model with perfect discriminating ability quantify the importance of each cortical region. This is the first time such a phenomenon is discovered and weights in cortical areas are precisely described in AD and its prodromal stages to the best of our knowledge. Our findings can establish other study models to differentiate the patterns in various diseases with cognitive impairments and help to identify the underlying pathology.

1. Introduction

Alzheimer's disease (AD) is a chronic irreversible neurodegenerative disease that starts insidiously and gradually worsens over time. It begins with mild cognitive decline and can progress to the aphasia and alterations in behavior. Nowadays, more than 29 million people worldwide are diagnosed with AD, and the number is projected to nearly triple by 2060 (Matthews, 2019). At present, AD is incurable and it commonly presents later in life. Scientists are exploring early intervention techniques in AD to prevent the disease from worsening. There are several hypotheses for the underlying pathology of AD. These include the genetic hypothesis, cholinergic hypothesis, amyloid hypothesis, and tau protein hypothesis (Bertram, 2019; Mesulam, 2019; Reddy, 2019; Busche, 2019). However, the cause of the disease is not fully known and the diagnosis depends heavily on the medical history, behavioural observations, and neuropsychological testing such as the commonly used mini-mental state examination (MMSE) (Pinto, 2019).

In contrast to more subjective diagnostic techniques, imageology provides advanced analysis for the in-depth observation of the human brain (Zhao, 2017; Sarraf, 2016; Wolk, 2017). Ryan et al. segmented the MRI images into gray matter, white matter and CSF, and computed their spearman correlations in the AAL template. The occipital lobe has been implicated as part of the cortical signature of cognitive impairment (O'Dell, 2019). Boyd et al. detected the disturbed cortical laminations of the medial temporal lobe in patients with AD (Kenkhuis, 2019). Keith et al. proved the volume of hippocampus was closely related to AD in a longitudinal study on the rate of hippocampal atrophy (Josephs, 2017). In addition to the research on morphology, functional connectivity in the

* Corresponding author.
E-mail address: jsheng@hdu.edu.cn (J. Sheng).

https://doi.org/10.1016/j.heliyon.2022.e08827
Received 8 July 2020; Received in revised form 29 April 2021; Accepted 19 January 2022

human brain has also attracted the attention of researchers (Passamonti, 2019; Hafkemeijer, 2017; Yamashita, 2019). Rather than structural changes in a single region of the brain, abnormal connectivity patterns are the underlying cause behind cognitive decline. Franzmeier et al. demonstrated that higher global left frontal cortex connectivity was the functional substrate for cognitive reserve that helped to maintain episodic memory relatively well in the early stages of AD (Franzmeier, 2017). Li et al. evaluated the connectivity covariance among different brain regions for mild cognitive impairment (MCI), AD and healthy controls (HC). There is a corresponding decrease in connectivity going from HC to MCI to AD, especially in the temporal lobe, occipital-parietal lobe and parietal-temporal lobe (Li, 2018). Until now, no consensus has been reached regarding which human brain cortical or subcortical area is the most affected in AD.

Machine learning makes it possible to assess the importance of each brain area by building classification models with emphasis on optimal regional weights. Recently, many researches have achieved high accuracies in recognition of AD patients through training learning models. Lyduine et al. investigated the W scores and discrimination maps for the binary classification of MCI and AD, and obtained 83.8% accuracy (Collij, 2016). Massimiliano et al. trained a support vector machine (SVM) model with radial-basis function kernel and demonstrated a performance for the recognition of MCI and AD with the area under curve (AUC) value of 0.82 (Grassi, 2019). Khazaee et al. proposed direct-graph based measures for the representation of functional connectivity in the cortex, and compared groups of machine learning algorithms in the binary classification of HC, MCI and AD (Khazaee, 2016; Khazaee, 2017; Hojjati, 2017). Various centralities from the adjacent connectivity matrix were computed in the putative 264 functional areas and an accuracy of 88.4% was obtained.

High accuracy in binary classification for HC, MCI or AD is of little significance in clinical neurocognitive evaluation. There would not be only two classifications of patients with cognitive disorders. It is very important to explore the method that can accurately discriminate multiple groups in different stages of MCIs and AD. Ramzan et al. proposed a deep learning approach for the multi-class classification of AD stages with high accuracies (Ramzan, 2020). The Alzheimer's Disease Neuroimaging Initiative (ADNI) tracks the progression of AD in the human brain with clinical, imaging and genetic biomarkers through the process of normal aging, early mild cognitive impairment (EMCI), late mild cognitive impairment (LMCI) to dementia or AD (Weiner, 2017). Previously, we proposed an effective classification method based on the multimodal parcellation HCP MMP, and nearly achieved 80% accuracy of any three groups among HC, EMCI, LMCI and AD through the SVM algorithm. In this study, the deep learning model GoogLeNet was improved to accommodate the ensemble input of structural, functional connectivity and functional topological modalities. Weights trained in the model were mapped into 360 cortical areas and achieved more than 95% recognition accuracy in four-group classification.

2. Materials and method

2.1. Data source

160 subjects including EMCI, LMCI, AD patients and healthy controls were downloaded from the ADNI2 database. To ensure the consistency and reproducibility of results in this study, only those subjects scanned by Philips were considered. Table 1 shows the basic statistical information of acquired subjects in this paper. Structural MRI with T1 weighting and functional MRI of resting-state were downloaded in the company of filed map information.

Table 1. Basic statistical information of acquired subjects.

	HC	EMCI	LMCI	AD
Total	43	53	34	30
Male: Female	16:27	20:33	21:13	12:18
Average	75.51	71.68	72.35	73.10
SD	6.27	6.39	8.26	6.81

2.2. Parcellation

There were three kinds of cortical parcellation atlas adopted in this study for the purpose of comparison: Desikan-Killiany atlas, DKT atlas, and a multimodal parcellation method proposed by HCP (HCP MMP). In the Desikan-Killiany atlas, 34 cortical regions of interest (ROIs) for each hemisphere were extracted, and in the DKT atlas, the number was 31. Both parcellations can be conveniently achieved by FreeSurfer with the subject's structural MRI data. Up until now, the HCP MMP provides the most fine-grained cortical parcellation with 180 areas in each hemisphere. Due to its multimodal-based preprocessing (dealing with structural MRI, functional MRI, connectivity and functional topological data) and strict scanning data requirement, the parcellation for the ADNI database was achieved by joint HCPMMP (JHCPMMP) method proposed by us (Sheng, 2019). Briefly, structural MRI data were first preprocessed into T1w space with FreeSurfer, and then functional MRI series were registered with structural MRI in fMRIprep software. Finally, both structural and functional MRI data were translated into CIFTI space in which 32,492 surface vertices per hemisphere and 26,298 subcortical voxels were defined.

2.3. Multimodal cerebral cortical measures

As a result of parcellation, all the vertices making up the cerebral cortex for each subject were divided into N areas. N equaled 62, 68 and 360 respectively for the DKT atlas, Desikan-Killiany atlas, and HCP MMP. Each subject was measured by multimodality: structural, functional connectivity and functional topological modalities. For structural modality, cortical thickness and curvature were considered as important roles in measuring morphological changes in the cerebral cortex for cognitive impairment and Alzheimer's disease. The shape of structural modality was $2 \times N$.

Functional connectivity was generated between any two regional fMRI series through computing the $N \times N$ correlation matrix or adjacent matrix in which ROIs in each atlas were defined as nodes and the correlation coefficients were used as the weights of edge. A dynamic proportion of the strongest weights (dPSW) was reserved to eliminate noise and spurious connectivity. Both weighting and binarizing processes were carried on this sparse $N \times N$ matrix.

For topological modality, Brain Connectivity Toolbox (BCT) was adopted for complex-network analysis of weighted and binary functional connectivity computed ahead. In weighted connectivity, seven regional measures including strength (S), clustering coefficient (CC), local efficiency (LE), betweenness centrality (BC), eigenvector centrality (EC), page-rank centrality (PC) and degree (D) were computed for each ROI in the cerebral cortex. In binary pattern, eight regional measures consisting of strength (S), clustering coefficient (CC), local efficiency (LE), betweenness centrality (BC), eigenvector centrality (EC), page-rank centrality (PC), k-coreness centrality (KC) and flow coefficient (FC) were computed. Overall, the shape of functional topological modality was $15 \times N$.

2.4. Multimodal deep learning

After the preparation of multimodal cerebral cortical measures, a deep learning procedure was implemented in Paddle-Paddle framework to achieve the recognition of different MCIs, AD patients and healthy controls. Sheng et al. proposed a JMMP-LRR method which combines the logistic regression-recursive feature elimination (LR-RFE) and JHCPMMP for three classifications of AD, MCI, and normal aging (Sheng, 2020). For compatibility with multimodality, the training model used in this study was adapted from one of the most successful deep learning networks:

GoogLeNet. Originally, GoogLeNet was designed for image recognition in computer vision, and it was the champion of the ImageNet Large Scale Visual Recognition Challenge 2014 (ILSVRC2014). In this study, the connectivity matrix was regarded as an $N \times N$ input to GoogLeNet, focusing on the discrimination of details in global brain connectivity among different groups. The unique structure 'Inception' which played the part of a fundamental component in GoogLeNet largely reduced the dimension of input as well as extracted the deep features through multi-kernel and multi-layer convolutions. The default shape of input in GoogLeNet is 224 × 224, while the structure of the network was modified to cater to the actual shape of connectivity in this study. More working principles and parameters of GoogLeNet can be found in the reference (Szegedy, 2014).

The key step of multimodal deep learning is to integrate various representations of data, which involves unifying dimensions and scales of different modalities. We designed a two-stage cascade concatenation for blending inputs. In GoogLeNet, outputs of convolutions and max-pooling were concatenated along the last axis, by default the axis would be the number of convolution kernels used in each inception. Accumulated with the stack of inception, the final number of concatenated outputs ended with 1024 × 1, which represents the 'learnt' deep features corresponding to the original $N \times N$ input. For structural and functional topological modalities, inputs were directly merged along the first dimension, thus the shape of integrated modalities was $17 \times N$. In order to integrate with the functional modality data, the $17 \times N$ matrix was flattened into $(17 \times N) \times 1$ array. Consequently, the shape of the two-stage cascade concatenation was $(17 \times N + 1024) \times 1$. It would be (2,078 × 1), (2,180 × 1) and (7,144 × 1) for the DKT atlas, Desikan-Killiany atlas and HCP MMP respectively.

Data segmentation was also a key process in deep learning. In this study, we separated data into training and test sets and kept the ratio of those as 4:1. The batch size was set to be 8, and the number of epochs was 13. Based on these conditions, the total number of steps reached was 208. Group normalization (GN) was implemented before training. Different from global normalization or batch normalization, GN was able to restrict the scale of samples at the group level rather than covering up the subtle changes among cognitive impairment patients.

Multi-class recognition was considered as a possibility estimation for each group in this study, thus the SoftMax activation function was employed to map the learning result to a probability value. Eqs. (1), (2), (3) shows how to assign the probability.

$$Y_i = \sum_{j=1}^{17 * N+1024} w_j^T x_j + b \tag{1}$$

$$P_i = e^{y_i} \Big/ \sum_{j=1}^{(17* N+1024)} e^{y_j} \tag{2}$$

$$\sum_{i=0}^{\text{the number of classes}} P_i = 1 \tag{3}$$

where, i is the number of classes, in this study, $i = 4$, representing EMCI, LMCI, AD and HC, j is the number of deep learning features, here it is $(17 \times N + 1024)$.

For the multimodal inputs, two-stage cascade concatenation resulted in x_j. Adding each x_j multiplied by a given weight w_j with a fixed offset b, the output Y_i depicts the contribution of each deep feature. Essentially, the problem of classification is to find the appropriate weight for each cortical area. In SoftMax function, P_i was assigned by Eq. (2), and the sum of all the probabilities is 1.

3. Results

The working diagram is illustrated in Figure 1A. Figure 1B shows the two-stage cascade concatenation of multimodal inputs in the deep learning module. 160 subjects in four groups were first preprocessed and parcellated by three cortical atlases. Structural, functional connectivity and topological functional measures were extracted and computed in those parcellated ROIs as a representative of multimodality in each subject cerebral cortex. All the subjects were divided into training and testing sets. Each modality was inputted into the deep learning module, going through the neural network, and was concatenated as a whole input to SoftMax function. Four-class recognition was iteratively optimized through the performance of the model trained.

Figure 2 shows the comparison of training accuracy in different cortical atlases. Figure 2A-C are processes of training with structural modality in HCP MMP, Desikan-Killiany atlas and DKT atlas respectively.

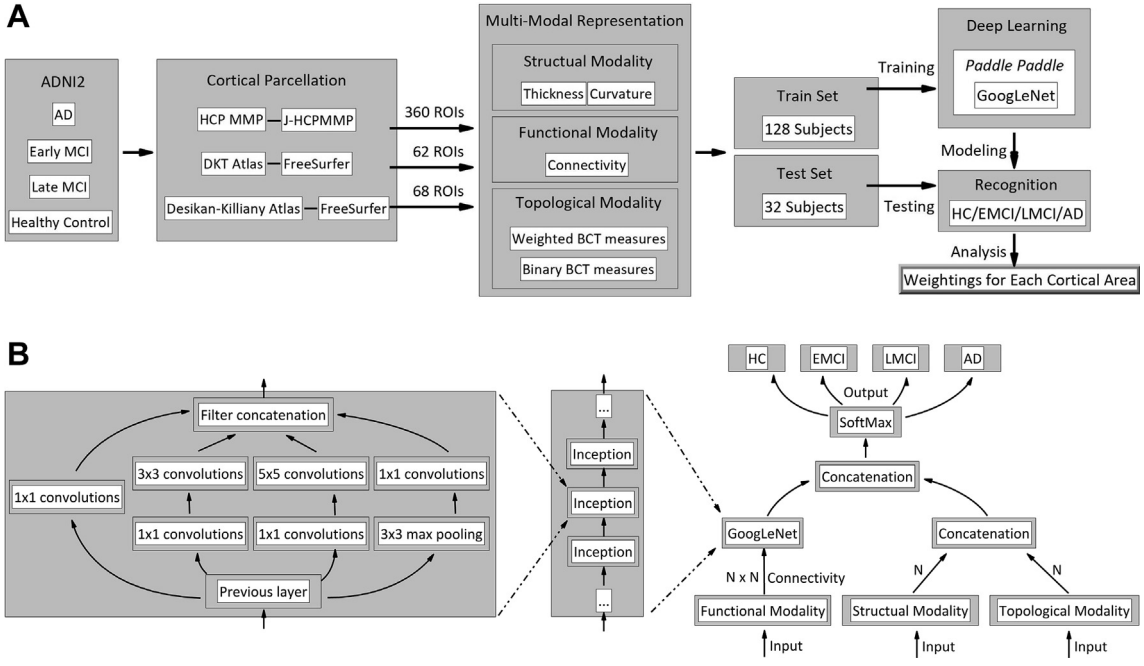

Figure 1. (A) Multimodal analysis method proposed in this study; (B) Multimodal deep learning module.

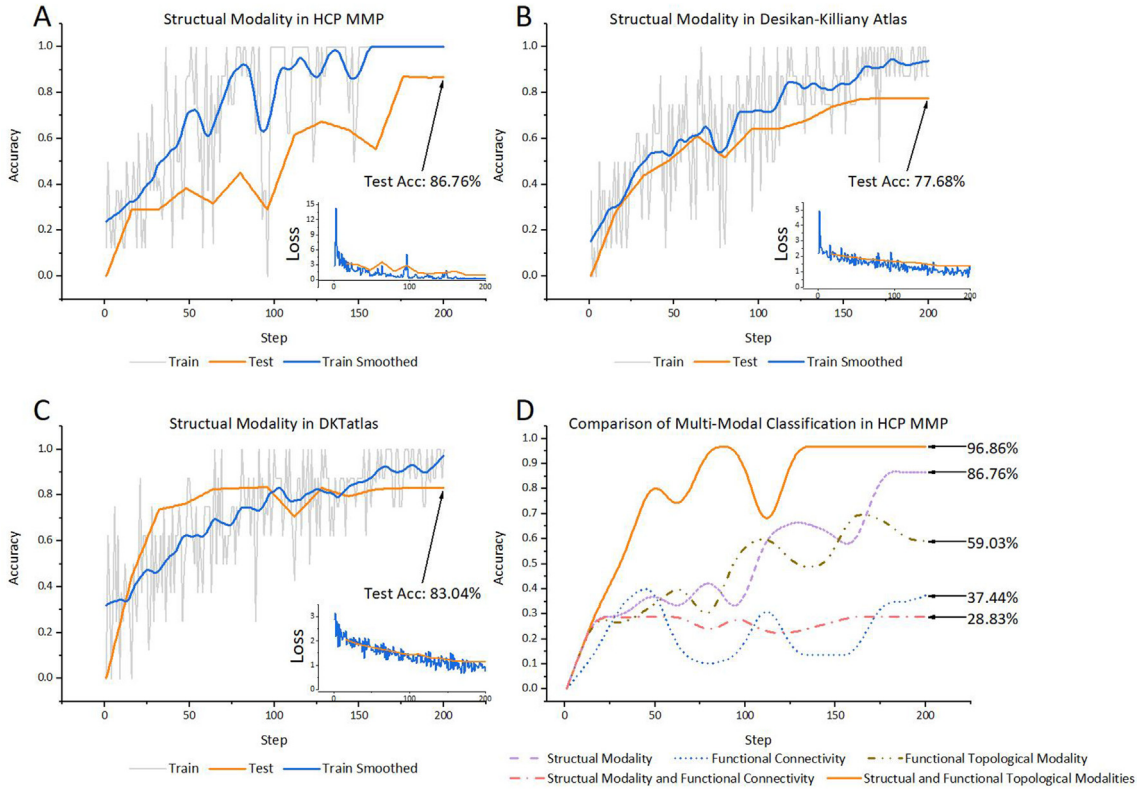

Figure 2. Comparison of training accuracy in different cortical atlases.

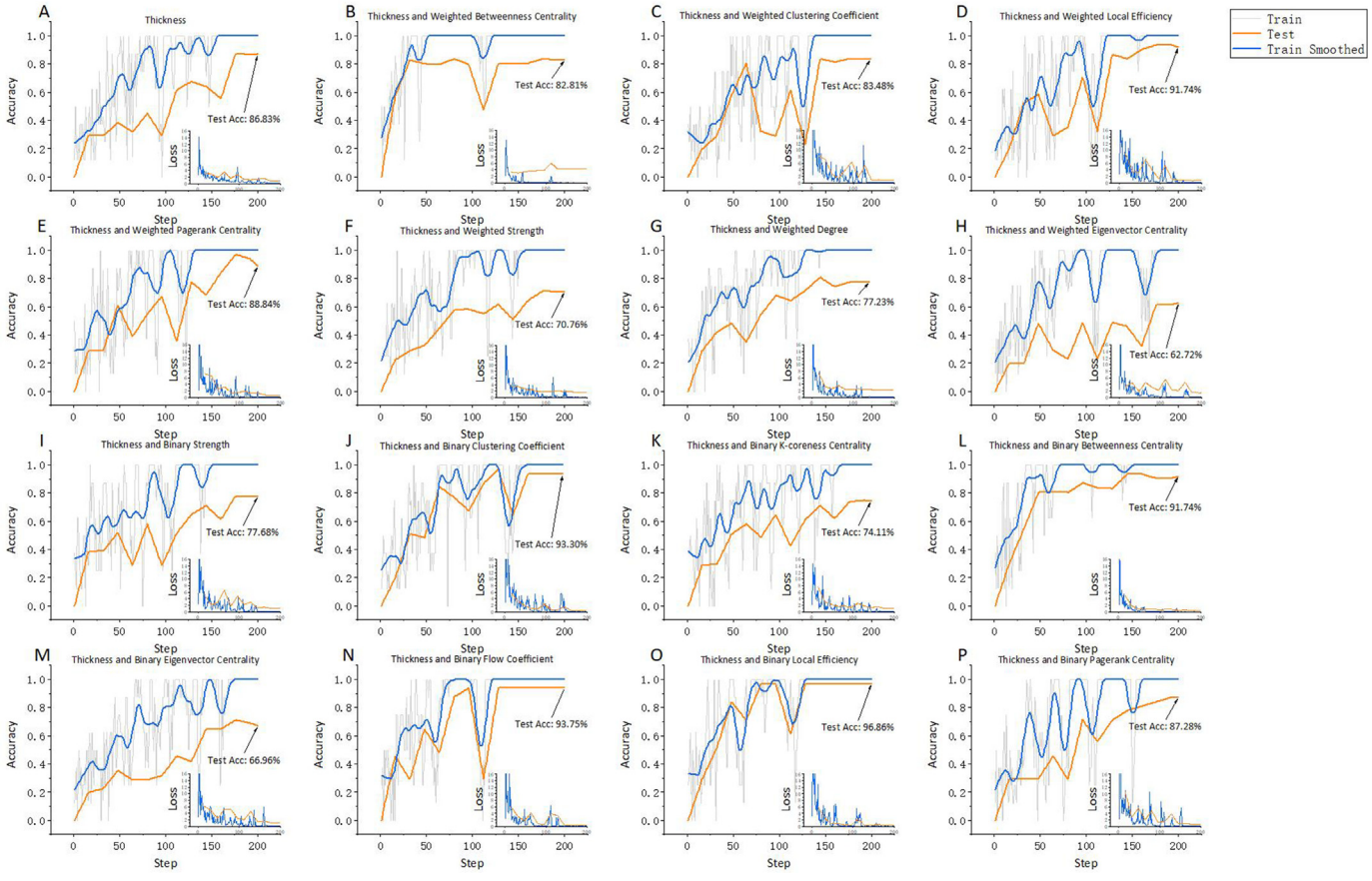

Figure 3. Classification performance in the ensemble of structural and functional topological modalities.

The blue curve represents the smoothed changes in training accuracy, and the curve in orange is the actual value of testing accuracy during steps. By comparison, the classification accuracy in HCP MMP gets the best testing performance of 86.76%, followed by DKT atlas, and the last is Desikan-Killiany atlas. The subgraph at the bottom right in each figure is the loss value in function with steps, from which loss in HCP MMP shows the fastest decline. For multimodal classification comparison in HCP MMP, Figure 2D shows the smoothed testing results of various combinations of structural, functional and functional topological modalities. It can be observed that the ensemble of structural and functional topological modalities reaches the highest score in testing accuracy at 96.86%, followed by 86.76% in the structural modality, 59.03% in the functional topological modalities, 37.44% in the functional modality, and 28.83% in the ensemble of structural and functional modalities.

Figure 3 shows the contrastive analysis of classification performance in the ensemble of structural and functional topological modalities. For the input of functional topological modalities, there are seven weighted and eight binary network measures computed in this study. Thus, Figure 3A is the classification result with cortical thickness for comparison. Fig.3B-H is the result of the ensembles of thickness with weighted BC, CC, LE, PC, S, D and EC respectively. Fig.3I-P is the result of the ensembles of thickness with binary S, CC, KC, BC, EC, FC, LE and PC respectively. Among all these results, the ensemble of thickness with binary local efficiency reaches the highest classification accuracy of 96.86%. The changes of train and test performance during learning here are used to illustrate the convergence speed in each model. The steeper the curve is, the faster the model converges. Thus, in addition to the highest classification accuracy shown in Fig.3O, the model is the most accurate compared with others. Furthermore, the smallest distance between training and testing curves in Fig.3O indicates the lowest risk of overfitting. Table 2 lists the confusion matrix and classification performance for each category corresponding to the model in Fig.3O.

Four models were trained by using the modalities of structural and functional topological in HCP MMP for the HC/EMCI/LMCI/AD recognition. Figure 4 illustrates the changing process of model trained varying with steps for the recognition in AD patients. Weights in the model are mapped onto 360 HCP MMP cortical areas. The red color represents positive weights and the blue represents the negative. The first two rows are lateral and medial views for the left hemisphere, and the last two are those for the right. Each column is the resulting model and its classification accuracy within a training step. In the beginning, values of weights are assigned randomly. After the first step of training, the distribution of weights can be roughly observed even though the result is in no sense of high accuracy. With the increasing number of steps in training, the distribution of the weights is more stable and changes subtly. Training accuracy reaches 100% when there are around 100 steps.

Figure 5A shows the final trained model with weights mapped for multi-class classification in lateral and medial views. As mentioned above, the color red represents positive weights and the blue represents the negative. To clearly observe the weight emphasis of each cortical area, in Figure 5B, all the negative weights are changed to absolute values, and weights of 70% are retained. Color in red means a more substantial weight in the model. For both Fig.5A and Fig.5B, columns are mapped in model weights for HC, EMCI, LMCI and AD groups. With the deterioration of cognition, the cingulate cortex area becomes more important (or substantial) in the classification model, especially in the right hemisphere when observed in the medial view.

Figure 6 shows the final trained model for HC/EMCI/LMCI/AD classification in the anterior view of the frontal lobe with weights mapped. It can be observed that with the evolution of cognitive impairment, more cortical areas are involved in the related cognitive classification model; the large weights present a concentrated state, and drifts to the upper part of the frontal lobe.

Table 2. Confusion matrix and classification performance comparison.

		True			
		HC	EMCI	LMCI	AD
Prediction	HC	9	0	0	0
	EMCI	0	8	0	0
	LMCI	0	0	6	0
	AD	0	0	1	8
		Accuracy	**Precision**	**Recall**	**F1 Score**
Classification Performance	HC	100%	1.0	1.0	1.0
	EMCI	100%	1.0	1.0	1.0
	LMCI	96.8%	1.0	0.86	0.92
	AD	96.8%	0.89	1.0	0.94

4. Discussion

Various parcellation atlases based on structural, functional connectivity and functional topological cerebral cortical measures were analyzed and modeled for multi-class recognition in this study. A multimodal deep learning network was reformed to adapt to the complicated meaning and shape of input. The ensemble of thickness with binary local efficiency modalities was found to be the optimum feature combination for the HC/EMCI/LMCI/AD classification.

Desikan-Killiany and DKT are the most commonly used cortical atlases in neuroscience, while there are only 62 or 68 ROIs extracted for bilateral hemispheres. Limited parcellation restricts the ability to explore which areal feature takes the impact on cognitive impairment, and is the reason why the majority of research failed to achieve high recognition results in multi-group classifications. Since the fine-grained multimodal parcellation HCP MMP was proposed, it facilitates the study of more refined functional areas that are cognition related. In Fig.2A-C, the model in HCP MMP has the fastest convergence speed and the highest training and testing accuracies. The training stays constant at around 160 steps with the loss value dropping sharply throughout the iterations. While at the same steps for Desikan-Killiany and DKT atlases, models do not converge on a stable level and the values of training fluctuate greatly. Meanwhile, classification accuracies are not as high as HCP MMP are. Therefore, the follow-up experiments shown in Figure 2D were based on the multimodal cortex analysis in HCP MMP.

In other studies (Zhang, 2012; Sun, 2019; Hett, 2018), multimodal research which usually combines MRI with PET, CSF or genetic information have only regarded MRI as a single modality instead of exploring the relevancy among structural, functional connectivity and functional topological characteristics in MRI. Significant alterations in the structure of the cerebral cortex often lead to dysfunctions of connectivity between areas. It has been proved that the topology in connectivity contributes to the normal work of brain (Yu, 2016). From Figure 3, cortical thickness is observed as the most sensitive feature in identifying cognitive impairment. The training accuracy reaches the highest value with functional topological modality. In addition, performances of binary functional topological measures are better than the weightings, which mean that binarization helps to reduce the spurious connectivity and noise instead of causing information loss. The ensembles of thickness with binary clustering coefficient (Figure 3J), betweenness centrality (Fig.3L), flow coefficient (Fig.3N) and local efficiency (Fig.3O) obtain more than 0.9 accuracy. It is consistent with the previous studies that local consistency and centrality are often used to measure whether the transmission of areal signals functions normally, and these network measures are important and effective functional topological indicators for the measuring of brain functional connectivity.

Deep learning omits the explicit time-consuming feature selection. Almost all conventional machine learning methods require selection of inputs or their combination will result in better performance in classification no matter the filter or wrapper strategy implemented. In this study, multimodal data were directly inputted into the reformed deep learning and their weights approach the truth in iterations. Previously,

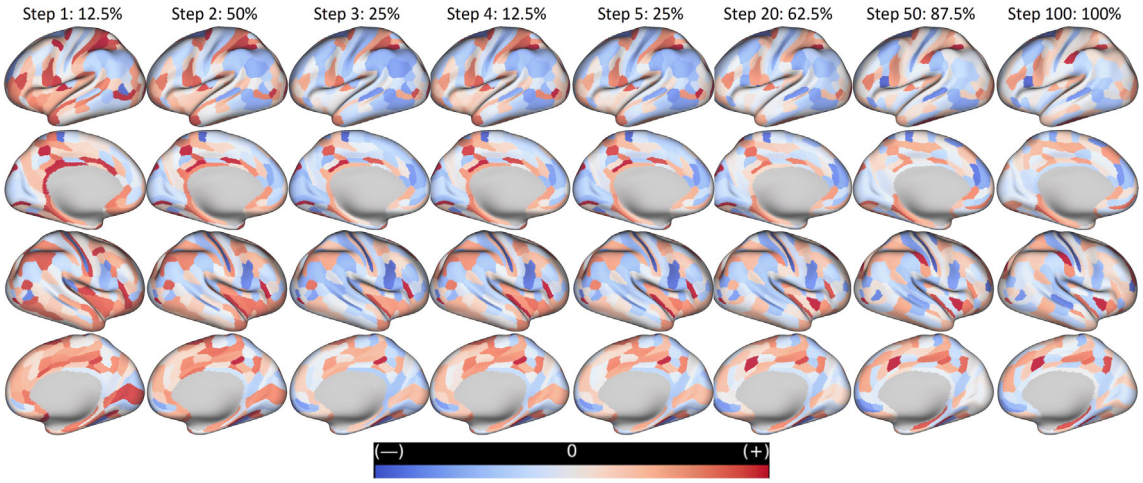

Figure 4. Changing weights in each HCP MMP area during training for the AD patient's recognition.

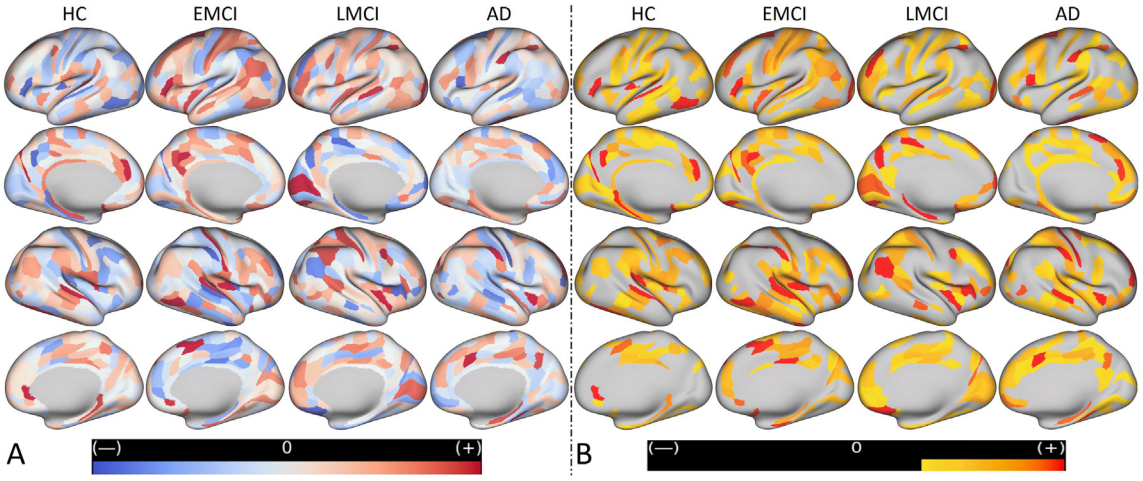

Figure 5. (A) Weights in the final model for multi-class classification. (B) The absolute value of A), 30% of the lowest weights in model are eliminated.

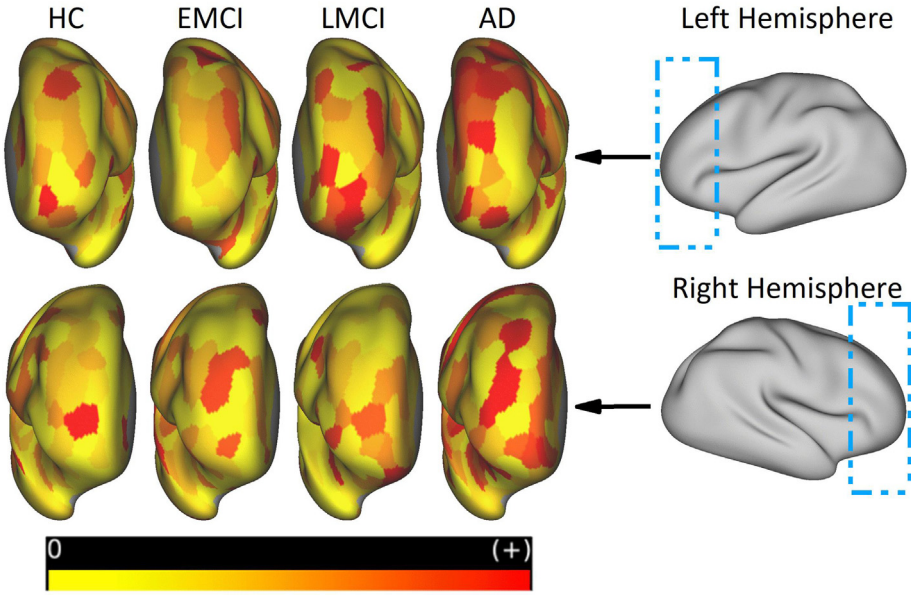

Figure 6. Mapped weights for HC/EMCI/LMCI/AD in anterior view of the frontal lobe. The upper row is for the left hemisphere, and the bottom row is for the right. Absolute weights of the multi-class classification model are all reserved.

Table 3. Comparison with major state of AD classification studies.

Study	Sample size	Classification	Accuracy
Wang (2021)	120	Binary-group	100%
Mehmood (2021)	300	Binary-group	98.7%
Sharma (2021)	509	Binary-group	86.7%
Yang (2020)	79	Binary-group	80.8%
Wu (2020)	42	Binary-group	77.5%
Janghel (2020)	54	Binary-group	99.9%
Mutahari (2020)	200	Binary-group	86.0%
Sheng (2019)	96	Binary-group	95.8%
This study	**160**	**Four-group**	**96.8%**

Table 4. Significant areas with greater weights in classification model.

HCP Area	Brodmann Area	Functional Network	Key Studies
PF cortex	BA 40	Ventral Attention	Chai (2019), Shan (2018)
L-d32	BA 32	Default Mode	Yokoi (2018), Chiaravalloti (2017)
R-p32pr			
L-5m	BA 5	Somatomotor	Jones (2019), Dong (2018)
R-MI	Middle Insular Area	Ventral Attention	Roquet (2017), Anor (2017)
R-Pres	BA 27	Visual	Parker (2019), Zhao (2019)

we attempted to find the optimal combination from thousands of candidate features such as SVM before any machine learning (Sheng, 2019). However, with the increasing scale of multimodal features, results of classification are very unstable and hard to be reproduced by the same random search strategy of feature selection.

Over 0.95 classification accuracy was obtained for multi-class recognition. Amoroso (2018) reported their random forest based deep neural network accomplished 38.8% for the recognition of four classes. That was just a few percentages higher than the baseline of 25%. Essentially, this is caused by the trained models which cannot reflect the subtle alterations among MCIs and AD, especially for the gap between EMCI and LMCI. We investigate some of the major state of art models used for diagnosis of AD and list the comparisons in Table 3. In this study, other groups of controlled experiments including the ensembles of thickness with binary flow coefficient (93.75%), thickness with binary clustering coefficient (93.30%), thickness with weighted local efficiency (91.74%) and thickness with binary betweenness centrality (91.74%) concurrently state the superior performance for the HC/EMCI/LMCI/AD recognition.

Weights mapping into the cortical areas express how much an areal feature can impact cognitive impairment. In Figure 4, the PF cortex (BA40) in the bilateral hemisphere are in dark red and the left BA44 area are dark blue in step 100. These areas are the most important two regions of the cerebral cortex that are linked to speech, which are named Wernicke's area (BA39 and BA40) and Broca's area (BA44 and BA45). Many researchers have proved these regions are closely responsible for the Alzheimer-related aphasia (Kurra, 2019; Whitfield, 2014; Iancheva, 2019). In addition to these two main regions, areas including Area L-d32 (BA32), Area L-5m (BA5), Area R-MI (Middle Insular Area), Area R-Pres (BA27), Area R-p32pr (BA32) show significant large weights in the AD recognition model. Studies from the Neurosynth (https://www.neurosynth.org/) report that these regions are highly correlated with human cognitive ability. Cera (2019) compared the functional connectivity (FC) patterns of the cingulate subregions (BA32) in a sample of mild cognitive impairment patients and healthy elderly subjects. They found that compared to MCI, the HC cohorts showed significant increased level of FC for the ventral part of the anterior cingulate cortex. Carlesimo (2015) tested the volumes of hippocampal subfields from 30 AD and 41 MCI patients, found a prevalent atrophy of the presubicular-subicular complex (BA27) from the early phases of AD and suggested atrophy in this area could be the earliest hippocampal anatomical marker of Alzheimer's disease. Table 4 lists the areas with greater weights in classification model and their locations in functional networks. These areas are mainly located in the ventral attention network, default mode network, somatomotor network and visual network. In Figure 5, the obvious drift of cognitive related regions can be observed in the prefrontal lobe and surrounding the cingulate area in the right hemisphere compared with the AD and HC absolute weights in the classification model. It is the first time such a phenomenon is discovered and weights in cortical areas are given exactly for Alzheimer's disease and its prodromal stages.

Several aspects can be improved in this study. First, the acquired 160 subjects were divided into a training set and testing set, and this may introduce overfitting to some extent. The trained model gradually tends to improve the accuracy of classification in the known testing set and results in losing the recognition ability in future samples. Therefore, as the number of samples increases, the dataset should be separated into three parts: training, validation, and testing. The testing set should not be used during training and validation procedures. Second, with the development of deep learning, more and more efficient neural network models are constantly proposed and applied in various research domains. Considering the continuity of cognitive impairment and its gradual pathological process, longitudinal modality in the fMRI series should be available features as the input to the recurrent neural network.

Clinically, this machine learning would be very helpful in identifying people who are at the early stages of cognitive impairment. Usually, patients are identified when they have already had significant neurodegeneration. Early detection through this method is accomplished by non-invasive methods. Currently, cerebrospinal fluid (CSF) sampling for biomarkers and positron emission tomography (PET) scans are commonly used to diagnose patients with cognitive impairments, especially if there is a question about whether AD is the true underlying pathology. Those methods are limited by cost as well as discomfort to the patient. In current practice, machine learning on already available MRI data may prevent the need for more expensive or invasive testing. In addition, this can identify a wider network of people which would be not only impactful in the inclusion of more participants in clinical trials, but also help evaluate for other contributors which could potentially be adjusted (underlying depression, high-risk medications). Clinical trials often fail to demonstrate benefit in AD. This challenge arises from the fact that when the disease reaches the clinically apparent phase, the trial medications may not be as effective as they would be in patients who are in the preclinical or prodromal phases. In addition, cognitive impairments are a manifestation of many neurodegenerative disorders such as frontotemporal dementia and Lewy body dementia.

5. Conclusion

To reveal the structural, functional connectivity and functional topological relationships among different stage of MCIs and AD patients in this paper, 160 subjects in EMCI, LMCI, AD and HC were acquired from ADNI2 and a novel method was proposed for the analysis of regional importance with an improved deep learning model. Obvious drift of cognitive related regions can be observed in the prefrontal lobe and surrounding the cingulate area in the right hemisphere when comparing AD and HC absolute weights in the classification model. It is in consensus with previous reports that the alterations of these regions are responsible for cognitive impairment. Different parcellation atlases of the human cerebral cortex were compared, and the fine-grained multimodal parcellation HCPMMP performed the best with 180 cortical areas per hemisphere. In multi-group classification, the highest accuracy was 96.86% with the ensemble of structural and functional topological modalities as input to training model. Weights in the trained model with perfect discriminating ability quantify the importance of each cortical

region. This is the first time such a phenomenon is discovered and weights in cortical areas are given exactly for AD and its prodromal stages as far as we know.

Our multi-model deep learning method demonstrates the functionality of the human brain and the topographical connections between different areas of the human neuroanatomy, and identifies patterns in patients with EMCI, LMCI and AD. Future models can potentially help to specify the underlying pathology in a patient with cognitive impairments using patterns found in the different disease processes. Based on our findings, other study models can be established to differentiate the patterns in various diseases with cognitive impairments and help to identify the underlying pathology.

Declarations

Author contribution statement

Jinhua Sheng: Conceived and designed the experiments; Contributed reagents, materials, analysis tools or data; Wrote the paper.

Bocheng Wang: Performed the experiments; Analyzed and interpreted the data; Wrote the paper.

Qiao Zhang, Margaret Yu: Analyzed and interpreted the data.

Funding statement

This work was supported by the National Natural Science Foundation of China (No. 61871168).

Data availability statement

All key datasets generated and analyzed during this study are included in this manuscript. The raw datasets are also available on reasonable request.

Declaration of interests statement

The authors declare no conflict of interest.

Additional information

No additional information is available for this paper.

References

Amoroso, N., 2018. Deep learning reveals Alzheimer's disease onset in MCI subjects: results from an international challenge. J. Neurosci. Methods 302, 3–9.
Anor, C.J., 2017. Neuropsychiatric symptoms in Alzheimer disease, vascular dementia, and mixed dementia. Neurodegener. Dis. 17, 127–134.
Bertram, L., 2019. Alzheimer disease risk genes: 29 and counting. Nat. Rev. Neurol. 15 (4), 191.
Busche, M.A., 2019. Tau impairs neural circuits, dominating amyloid-β effects, in Alzheimer models in vivo. Threshold 30 (40), 50.
Carlesimo, G.A., 2015. Atrophy of Presubiculum and Subiculum Is the Earliest Hippocampal Anatomical Marker of Alzheimer's Disease, Alzheimer's & Dementia: Diagnosis, Assessment & Disease Monitoring, 1, pp. 24–32.
Cera, N., 2019. Altered cingulate cortex functional connectivity in normal aging and mild cognitive impairment. Front. Neurosci. 13, 857.
Chai, Y.L., 2019. Lysosomal cathepsin D is upregulated in Alzheimer's disease neocortex and may be a marker for neurofibrillary degeneration. Brain Pathol. 29, 63–74.
Chiaravalloti, A., 2017. Functional correlates of TSH, fT3 and fT4 in Alzheimer disease: a F-18 FDG PET/CT study. Sci. Rep. 7, 6220.
Collij, L.E., 2016. Application of machine learning to arterial spin labeling in mild cognitive impairment and alzheimer disease. Radiology 281 (3), 865–875.
Dong, C., 2018. Altered functional connectivity strength in informant-reported subjective cognitive decline: a resting-state functional magnetic resonance imaging study, Alzheimer's & Dementia: Diagnosis. Assess. Dis. Monitor. 10, 688–697.
Franzmeier, N., 2017. For the Alzheimer's Disease Neuroimaging Initiative (ADNI). Left frontal cortex connectivity underlies cognitive reserve in prodromal Alzheimer disease. Neurology 88 (11), 1054–1061.
Grassi, M., 2019. A clinically-translatable machine learning algorithm for the prediction of Alzheimer's disease conversion: further evidence of its accuracy via a transfer learning approach. Int. Psychogeriatr. 31 (7), 937–945.
Hafkemeijer, A., 2017. A longitudinal study on resting state functional connectivity in behavioral variant frontotemporal dementia and Alzheimer's disease. J. Alzheim. Dis. 5 (2), 521–537.
Hett, K., 2018. Multimodal Hippocampal Subfield Grading for Alzheimer's Disease Classification. Neuroscience. Available from:
Hojjati, S.H., 2017. Initiative ADN, others. Predicting conversion from MCI to AD using resting-state fMRI, graph theoretical approach and SVM. J. Neurosci. Methods 282, 69–80.
Iancheva, D., 2019. Functional MRI correlations between fatigue and cognitive performance in patients with relapsing remitting MS. Front. Psychiatr. 10, 754.
Janghel, R.R., 2020. Deep convolution neural network based system for early diagnosis of alzheimer's disease. IRBM. S195903182030110X.
Jones, S.A., 2019. Altered frontal and insular functional connectivity as pivotal mechanisms for apathy in Alzheimer's disease. Cortex 119, 100–110.
Josephs, K.A., 2017. Rates of hippocampal atrophy and presence of post-mortem TDP-43 in patients with Alzheimer's disease: a longitudinal retrospective study. Lancet Neurol. 16 (11), 917–924.
Kenkhuis, B., 2019. 7T MRI allows detection of disturbed cortical lamination of the medial temporal lobe in patients with Alzheimer's disease. Neuroimage: Clin. 21, 101665.
Khazaee, A., 2016. Application of advanced machine learning methods on resting-state fMRI network for identification of mild cognitive impairment and Alzheimer's disease. Brain Imag. Behav. 10 (3), 799–817.
Khazaee, A., 2017. Classification of patients with MCI and AD from healthy controls using directed graph measures of resting-state fMRI. Behav. Brain Res. 322, 339–350.
Kurra, V., 2019. Diffusion fiber tractography on phonological loop with Logopenic aphasia tau pathology: fiber-specific white matter reductions in Alzheimer's disease,"is it a causal or casual link? J. Neurol. Sci. 405, 76–77.
Li, Q., 2018. Aberrant connectivity in mild cognitive impairment and alzheimer disease revealed by multimodal neuroimaging data. Neurodegener. Dis. 18 (1), 5–18.
Matthews, K.A., 2019. Racial and ethnic estimates of Alzheimer's disease and related dementias in the United States (2015–2060) in adults aged ≥65 years. Alzheimer's Dementia 15 (1), 17–24.
Mehmood, A., 2021. A transfer learning approach for early diagnosis of alzheimer's disease on MRI images. Neuroscience 460, 43–52.
Mesulam, M.M., 2019. Cortical cholinergic denervation in primary progressive aphasia with Alzheimer pathology. Neurology 92 (14), e1580–e1588.
Mutahari, S.M., 2020. COMPUTER-AIDED diagnosis OF ALZHEIMER'S disease using T-sum feature obtained from brain 18F-FDG PET image utilising support vector machine. Int. J. Appl. 13 (2), 1–8.
O'Dell, R., 2019. REGION-SPECIFIC atrophy as measured BY cortical gray matter volume IS associated with both regional and total cortical amyloid-beta burden IN cognitively normal individuals at risk for ALZHEIMER'S disease. Am. J. Geriatr. Psychiatr. 27 (3), S186–S187.
Parker, T.D., 2019. Hippocampal subfield volumes and pre-clinical Alzheimer's disease in 408 cognitively normal adults born in 1946. PLoS One 14, e0224030.
Passamonti, L., 2019. Neuroinflammation and functional connectivity in Alzheimer's disease: interactive influences on cognitive performance. BioRxiv 532291.
Pinto, T.C., 2019. Is the montreal cognitive assessment (MoCA) screening superior to the mini-mental state examination (MMSE) in the detection of mild cognitive impairment (MCI) and alzheimer's disease (AD) in the elderly? Int. Psychogeriatr. 31 (4), 491–504.
Ramzan, F., 2020. A deep learning approach for automated diagnosis and multi-class classification of alzheimer's disease stages using resting-state fMRI and residual neural networks. J. Med. Syst. 44, 37.
Reddy, P.H., 2019. Amyloid beta and phosphorylated tau-induced defective autophagy and mitophagy in alzheimer's disease. Cells 8 (5), 488.
Roquet, D., 2017. Insular atrophy at the prodromal stage of dementia with Lewy bodies: a VBM DAR^{TEL} study. Sci. Rep. 7, 1–10.
Sarraf, S., 2016. DeepAD: alzheimer' s disease classification via deep convolutional neural networks using MRI and fMRI. BioRxiv, 070441.
Shan, Y., 2018. Neuronal Specificity of Acupuncture in Alzheimer's Disease and Mild Cognitive Impairment Patients: a Functional MRI Study, Evidence-Based Complementary and Alternative Medicine, 2018, p. 7619197.
Sharma, R., 2021. FAF-DRVFL: fuzzy activation function based deep random vector functional links network for early diagnosis of Alzheimer disease. Appl. Soft Comput. 106, 107371.
Sheng, J., 2019. A novel joint HCPMMP method for automatically classifying Alzheimer's and different stage MCI patients. Behav. Brain Res. 365, 210–221.
Sheng, J., 2020. Alzheimer's disease, mild cognitive impairment, and normal aging distinguished by multi-modal parcellation and machine learning. Sci. Rep. 10 (1), 1–10.
Sun, N., 2019. Multi-modal latent factor exploration of atrophy, cognitive and tau heterogeneity in Alzheimer's disease. Neuroimage 201, 116043.
Szegedy, C., 2014. Going Deeper with Convolutions arXiv:14094842 [cs] [Internet]. Available from: http://arxiv.org/abs/1409.4842.
Wang, Y., 2021. Assisted diagnosis of alzheimer's disease based on deep learning and multimodal feature fusion. Complexity 2021, 1–10.
Weiner, M.W., 2017. The Alzheimer's Disease Neuroimaging Initiative 3: continued innovation for clinical trial improvement. Alzheimer's Dementia 13 (5), 561–571.
Whitfield, D.R., 2014. Assessment of ZnT3 and PSD95 protein levels in Lewy body dementias and Alzheimer's disease: association with cognitive impairment. Neurobiol. Aging 35 (12), 2836–2844, 2014.
Wolk, D.A., 2017. Medial temporal lobe subregional morphometry using high resolution MRI in Alzheimer's disease. Neurobiol. Aging 49, 204–213.

Wu, Y., 2020. Differences in cerebral structure associated with depressive symptoms in the elderly with alzheimer's disease. Front. Aging Neurosci. 12, 107.
Yamashita, K., 2019. Functional connectivity change between posterior cingulate cortex and ventral attention network relates to the impairment of orientation for time in Alzheimer's disease patients. Brain Imag. Behav. 13 (1), 154–161.
Yang, B.H., 2020. Classification of alzheimer's disease from 18F-FDG and 11C-PiB PET imaging biomarkers using support vector machine. J. Med. Biol. Eng. 40, 545–554.
Yokoi, T., 2018. Involvement of the precuneus/posterior cingulate cortex is significant for the development of Alzheimer's disease: a PET (THK5351, PiB) and resting fMRI study. Front. Aging Neurosci. 10, 304.
Yu, M., 2016. Different functional connectivity and network topology in behavioral variant of frontotemporal dementia and Alzheimer's disease: an EEG study. Neurobiol. Aging 42, 150–162.
Zhang, D., 2012. Multi-modal multi-task learning for joint prediction of multiple regression and classification variables in Alzheimer's disease. Neuroimage 59 (2), 895–907.
Zhao, W., 2019. Trajectories of the hippocampal subfields atrophy in the Alzheimer's disease: a structural imaging study. Front. Neuroinf. 13, 13.
Zhao, Y., 2017. In vivo detection of microstructural correlates of brain pathology in preclinical and early Alzheimer disease with magnetic resonance imaging. Neuroimage 148, 296–304.